

IMAGES OF CHAOS IN ATTITUDE DYNAMICS OF MULTI-SPIN SPACECRAFT AND GYROSTAT-SATELLITES

Anton V. Doroshin

Space Engineering Department,
Samara State Aerospace University
(National Research University),
SSAU, 34, Moskovskoe Shosse str.,
Samara, 443086, Russia
doran@inbox.ru
doroshin@ssau.ru

Chaotic aspects of attitude motion of multi-spin spacecraft and gyrostat-satellites are investigated with the help of the Melnikov method and Poincaré sections. Images of dynamical chaos are plotted for some cases of phase portrait forms corresponded to different values of dynamical parameters. The bifurcations of the chaotic regimes with the change of phase portrait forms are illustrated.

Keywords: Multi-Rotor System, Multi-Spin Spacecraft, Dual-spin Spacecraft, Gyrostat, Homoclinic Chaos, Polyharmonic Perturbations, Melnikov Function, Poincaré Map

1. Introduction. The study of spacecraft (SC) attitude dynamics aspects was and still remains one of the important problems of modern classical and space-flight mechanics [1-45], and especially interesting features can be found in the framework of the dynamical chaos initiations into the dynamics of multi-rotor SC.

The constructional multi-rotor scheme is used for many types of SC, including satellites with assemblies of reaction wheels and multi/dual-spin SC. Here, e.g., we can mention such famous space projects and platforms as “Intelsat” by Hughes Aircraft Company (the Intelsat II was first launched in 1966, but its 8th generation Intelsat VI was actual till 1991); also the very famous Hughes’ dual-spinner is the experimental tactical communications satellite TACSAT-I launched in 1969; the “Meteosat”-project (initiated by European Space Research Organization with the Meteosat-1 in 1977 and operated until 2007 with the Meteosat-7) also was constructed on the base of the dual-spin

configuration.

The spin-stabilized SC with mechanically despun antennas was applied in the framework of GEOTAIL (the collaborative mission of Japan JAXA/ISAS and NASA, within the program “International Solar-Terrestrial Physics”); the construction scheme with the despun antenna was used for Chinese communications satellites DFH-2 (STW-3, 1988; STW-4, 1988; STW-55, 1990). The well-known Galileo mission’s SC (launched on October 19, 1989 to visit Jupiter) was built as the dual-spinner (fig.1) [46]. Also, we ought to indicate the world’s most-purchased commercial communications satellites such as Hughes / Boeing HS-376 (fg.1) [47, 48]. These satellites have spun sections with propulsion systems, solar drums, and despun sections with the communications payloads and antennas. Very versatile dual-spin models also are the Hughes’ HS-381 (the Leasat project), HS-389 (the Intelsat project), HS-393 (the JCSat project).

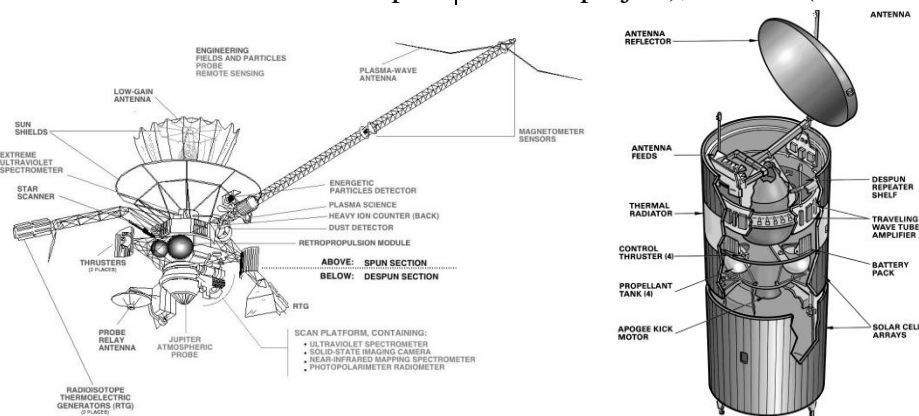


Figure 1. Examples of dual-spin spacecraft: Galileo and HS-376

The multi-rotor scheme can also correspond to the SC with assembles of reaction wheels, that is quite usual for real space projects. As first bright examples (fig.2) we can remember

such programs like the Hubble Space Telescope (HST) [49], the Kepler Space Telescope (KST) [50], and many others missions.

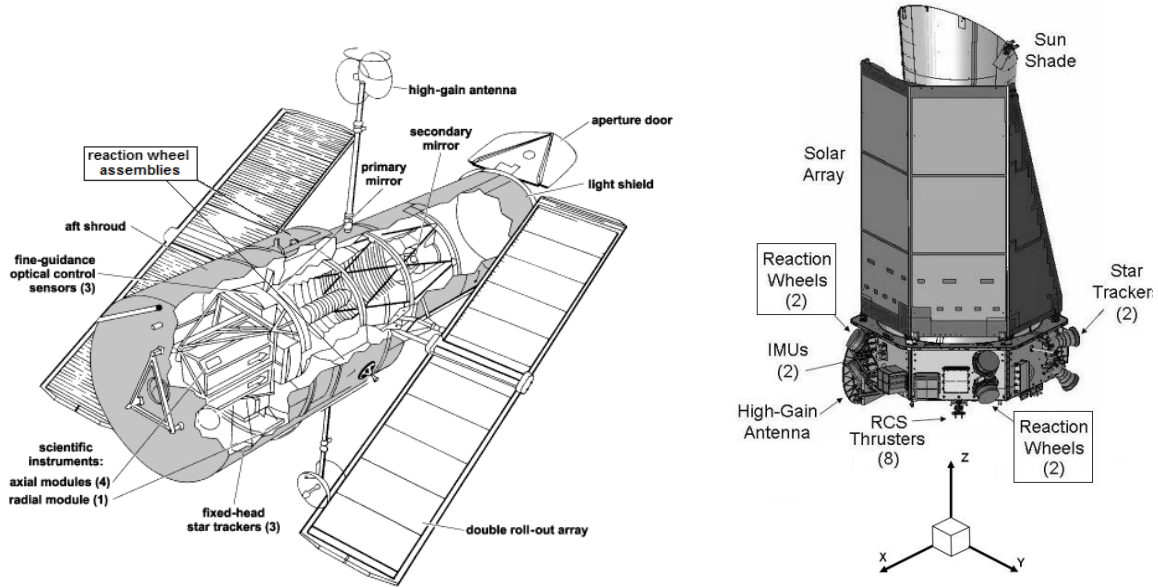


Figure 2. Examples of multi-rotor spacecraft with the reaction wheels assemblies: HST and KST

The fundamental results for the problem of the rigid body dynamics and for corresponding applied tasks in the framework of space flight mechanics are described, e.g. in [1-7] and in many other works. Also we must indicate the conjugated directions of research [8-45], including analytical/numerical modeling, analyzing the regular/chaotic regimes of motion of multi-body systems under the influence of external/internal perturbations. These are the analysis of the attitude dynamics of a dual-spin SC and gyrostats [8-17], the investigation of the multi-rotor systems and multi-spin SC dynamics [18-21], obtaining exact solutions [22-29], the chaotic dynamical aspects study [30-45].

2. The task formulation and mathematical models. Let us consider the attitude dynamics of multi-rotor (multi/dual-spin) SC [19] basing on the multi-body mechanical system (fig. 3) with using the hamiltonian formalism and the well-known Andoyer-Deprit canonical variables (fig. 4).

The Andoeyr-Deprit variable can be written

basing on the direction and the value of the system angular momentum vector \mathbf{K} as follows:

$$L = \frac{\partial T}{\partial \dot{i}} = \mathbf{K} \cdot \mathbf{k};$$

$$G = \frac{\partial T}{\partial \dot{\phi}_2} = \mathbf{K} \cdot \mathbf{s} = |\mathbf{K}| = K;$$

$$H = \frac{\partial T}{\partial \dot{\phi}_3} = \mathbf{K} \cdot \mathbf{k}'; \quad L \leq G$$

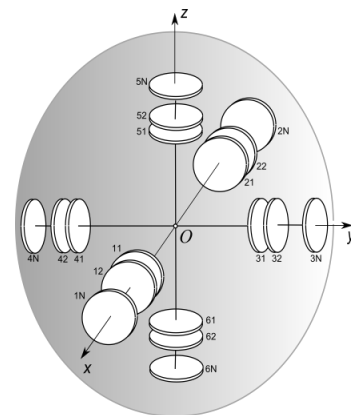


Figure 3. The multi-rotor mechanical structure of the multi-spin spacecraft

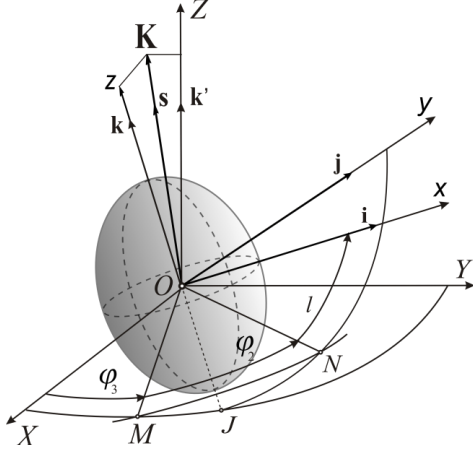


Figure 4. The Andoyer-Deprit canonical variables

The kinetic energy of the system has the following form in the Andoyer-Deprit canonical coordinates in the addition of angles of rotors' relative rotation $\xi_i = \langle l, \varphi_2, \varphi_3, \delta_{11}, \dots, \delta_{6N} \rangle$, and corresponding conjugated momentums $\Xi_i = \langle L, G, H, \Delta_{11}, \dots, \Delta_{6N} \rangle$ [19]:

$$\begin{aligned}
T = & (G^2 - L^2) \left[\frac{\sin^2 l}{\hat{A}} + \frac{\cos^2 l}{\hat{B}} \right] + \\
& + \frac{1}{\hat{C}} \left(L - \sum_{j=1}^N [\Delta_{5j} + \Delta_{6j}] \right)^2 - \\
& - 2\sqrt{G^2 - L^2} \left\{ \frac{\sin l}{\hat{A}} \cdot \sum_{j=1}^N [\Delta_{1j} + \Delta_{2j}] + \right. \\
& + \left. \frac{\cos l}{\hat{B}} \cdot \sum_{j=1}^N [\Delta_{3j} + \Delta_{4j}] \right\} + \\
& + \frac{1}{\hat{A}} \left(\sum_{j=1}^N [\Delta_{1j} + \Delta_{2j}] \right)^2 + \\
& + \frac{1}{\hat{B}} \left(\sum_{j=1}^N [\Delta_{3j} + \Delta_{4j}] \right)^2 + \sum_{j=1}^N \sum_{i=1}^6 \frac{\Delta_{ji}^2}{I_j}
\end{aligned} \quad (1)$$

where

$$\hat{A} = A - 2 \sum_{j=1}^N I_j; \quad \hat{B} = B - 2 \sum_{j=1}^N I_j; \quad \hat{C} = C - 2 \sum_{j=1}^N I_j;$$

and values A, B, C – are the main inertia moments of the main body, I_j – the axial inertia moments of rotors in the j -th layer (we assume the equivalence of the rotors in each layer).

Let us consider the case of the action of external torques with the small non-autonomous

potential

$$P = \mu \zeta(t) \cos \theta; \quad \mu \ll 1 \quad (2)$$

where θ designates the “restoring” angle.

This potential can describe the influence of external restoring torque from a weak magnetic field on the equatorial orbits at the regime of cylindrical precession of SC [29]. Also we will consider the polyharmonic form of the amplitude (it is actual practically in any case of the time-periodical amplitude and corresponds to the general form of the expansion in a Fourier series)

$$\zeta(t) = \sum_{n=0}^N \left[\bar{a}_n \sin(n\omega_p t) + \bar{b}_n \cos(n\omega_p t) \right]; \quad (3)$$

in the case when the “restoring” angle represents the angle between the angular momentum vector \mathbf{K} and longitudinal axis of the SC Oz (coinciding with the vector \mathbf{k} at the fig.4), and then the expression is actual

$$\cos \theta = L/G \quad (4)$$

The Hamiltonian of the system can be written in the form with general and perturbed parts

$$H = H_0 + \varepsilon H_1; \quad (5)$$

$$H_0 = T; \quad H_1 = \zeta(t)L$$

where the small parameters is equal $\varepsilon = \mu/G$. As it follows from the Hamiltonian (5) only one canonical pare (l, L) is positional, and other pares are cyclic; so it is enough to use two main dynamical equations in the form

$$\begin{cases} \dot{L} = f_L(l, L) + \varepsilon g_L; \\ \dot{l} = f_l(l, L) + \varepsilon g_l; \end{cases} \quad (6)$$

$$\begin{cases} f_L = -\frac{\partial H_0}{\partial l}; \quad f_l = \frac{\partial H_0}{\partial L}; \\ g_L = -\frac{\partial H_1}{\partial l}; \quad g_l = \frac{\partial H_1}{\partial L}; \end{cases}$$

Now we consider the motion regime when only equatorial rotors have non-zero summarized angular momentum, then it is possible to write constant blocks

$$\begin{cases} D_{12} = \sum_{j=1}^N [\Delta_{1j} + \Delta_{2j}] = 0, \\ D_{34} = \sum_{j=1}^N [\Delta_{3j} + \Delta_{4j}] = \text{const} \neq 0, \\ D_{56} = \sum_{j=1}^N [\Delta_{5j} + \Delta_{6j}] = 0, \end{cases} \quad (7)$$

This regime can describe the SC motion at the implementation of the attitude reorientation with acting transverse (equatorial) reaction wheels assemblies (like in the HST or KST at the fig.2). And in this case we have the following right-pars-functions of equations (6):

$$\begin{cases} f_l(l, L) = L \left[\frac{1}{\hat{C}} - \frac{\sin^2 l}{\hat{A}} - \frac{\cos^2 l}{\hat{B}} \right] + \frac{D_{34} L \cos l}{\hat{B} \sqrt{G^2 - L^2}}; \\ f_L(l, L) = (G^2 - L^2) \left(\frac{1}{\hat{B}} - \frac{1}{\hat{A}} \right) \sin l \cos l - \\ - \frac{D_{34}}{\hat{B}} \sqrt{G^2 - L^2} \sin l; \quad g_l(t) = \zeta(t); \quad g_L(t) \equiv 0; \end{cases} \quad (8)$$

3. The Melnikov function evaluation. In the purpose of the exact detection of homoclinic chaos initiation in the system at acting periodical perturbations we should prove the existence of simple zero-roots of the Melnikov function:

$$M(\vartheta) = \int_{-\infty}^{+\infty} \left[f_L(l(t), L(t)) g_l(t + \vartheta) - f_l(l(t), L(t)) g_L(t + \vartheta) \right]_{\{\bar{l}(t), \bar{L}(t)\}} dt \quad (9)$$

where the designation $\{\bar{l}(t), \bar{L}(t)\}$ implies evaluation of the integral along the homoclinic orbit.

Taking into account correspondences [19] between the Andoyer-Deprit variables and components of the angular velocity of the main body (p, q, r) , the Melnikov function (9) in our case is reduced to the expression:

$$M(\vartheta) = \int_{-\infty}^{+\infty} \left(\frac{1}{\hat{B}} - \frac{1}{\hat{A}} \right) \hat{A} p(t) (\hat{B} q(t) + D_{34}) \zeta(t + \vartheta) dt \quad (10)$$

where the exact analytical expressions for $p(t)$ and $q(t)$ along the homoclinic orbit are obtained in [19] – there is not any necessity to repeat them; but we must show the qualitative form of this time-dependencies (fig.5). From this qualitative form **the Statement 1** follows:

the time-function $p(t)$ is damped to zero odd function, $q(t)$ is even function, and, as the multiplication result, the block

$p(t)(\hat{B}q(t) + D_{34})$ is the damped to zero odd time-function.

Also with the help of the polyharmonic shape (3) and using trigonometric transformations we can obtain the multiplier $\zeta(t + \vartheta)$ in the form which contains explicit time-blocks and ϑ -phase-blocks separately:

$$\begin{aligned} \zeta(t + \vartheta) &= \quad (11) \\ &= \cos(n\omega_p t) \sum_{n=0}^N \left[\bar{a}_n \sin(n\omega_p \vartheta) + \bar{b}_n \cos(n\omega_p \vartheta) \right] + \\ &+ \sin(n\omega_p t) \sum_{n=0}^N \left[\bar{a}_n \cos(n\omega_p \vartheta) - \bar{b}_n \sin(n\omega_p \vartheta) \right] \end{aligned}$$

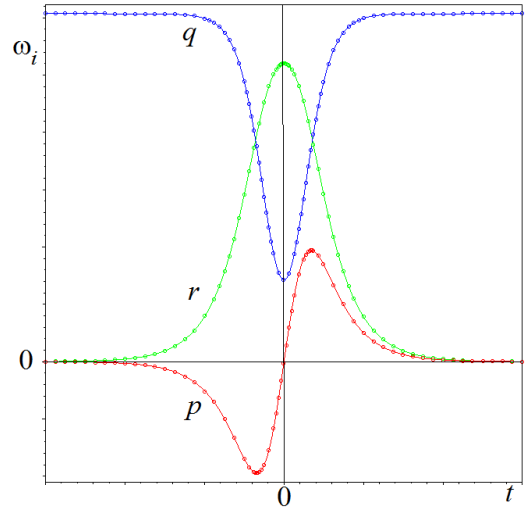


Figure 5. The qualitative form of time-dependencies for the angular velocity components along homoclinic orbit

Taking into account the *Statement 1* and the expression (11) (with understanding odd/even-functions properties), the integration gives the following polyharmonic result for the Melnikov function

$$M(\vartheta) = \sum_{n=0}^N \left[a_n \cos(n\omega_p \vartheta) - b_n \sin(n\omega_p \vartheta) \right] \quad (12)$$

with recalculated constant coefficients:

$$a_n = \Im \hat{A} \left(\frac{1}{\hat{B}} - \frac{1}{\hat{A}} \right) \bar{a}_n; \quad b_n = \Im \hat{A} \left(\frac{1}{\hat{B}} - \frac{1}{\hat{A}} \right) \bar{b}_n;$$

$$\Im = \int_{-\infty}^{+\infty} p(t) (\hat{B} q(t) + D_{34}) \sin(n\omega_p t) dt = \text{const} \neq 0$$

So, from the polyharmonic shape of the Melnikov function **the Statement 2** follows: *the Melnikov function in the considered case has infinite quantity of simple zero-roots, and*

then the homoclinic chaos initiation is inevitable.

This fact must be taken into engineers' attention at the space mission preparation and at the choice of working areas of SC dynamical parameters.

4. Numerical modeling of chaotic regimes.

For illustrating of the proved fact of the chaos initiation it is possible to provide a series of numerical experiments in the Poincaré sections/maps plotting basing on the "main-phase-repetition" condition: $(\omega_p t \bmod 2\pi) = 0$.

Let us define e.g. the following set of the polyharmonic perturbation coefficients:

$$\bar{a}_1 = 0.25; \quad \bar{a}_3 = 1.25; \quad \bar{a}_5 = 5; \quad (13)$$

$(\bar{a}_i = \bar{b}_j = 0 \forall j; i \neq \{1, 3, 5\})$ and the main frequency numerical value: $\omega_p = 0.75$.

As can we see from the modeling results, the chaotic layers are generated near the homo/heteroclinic bundles. These chaotic layer are generated as the result of multiple intersections of stable and unstable splitted manifolds of homo/heteroclinic orbits. Inside such chaotic layer any phase trajectory perform complex "chaotic" evolutions with variable characteristics of the dynamical regime – this is one of the main reasons of the SC complex abnormal oscillations, tilting irregular motions, and space missions malfunctions.

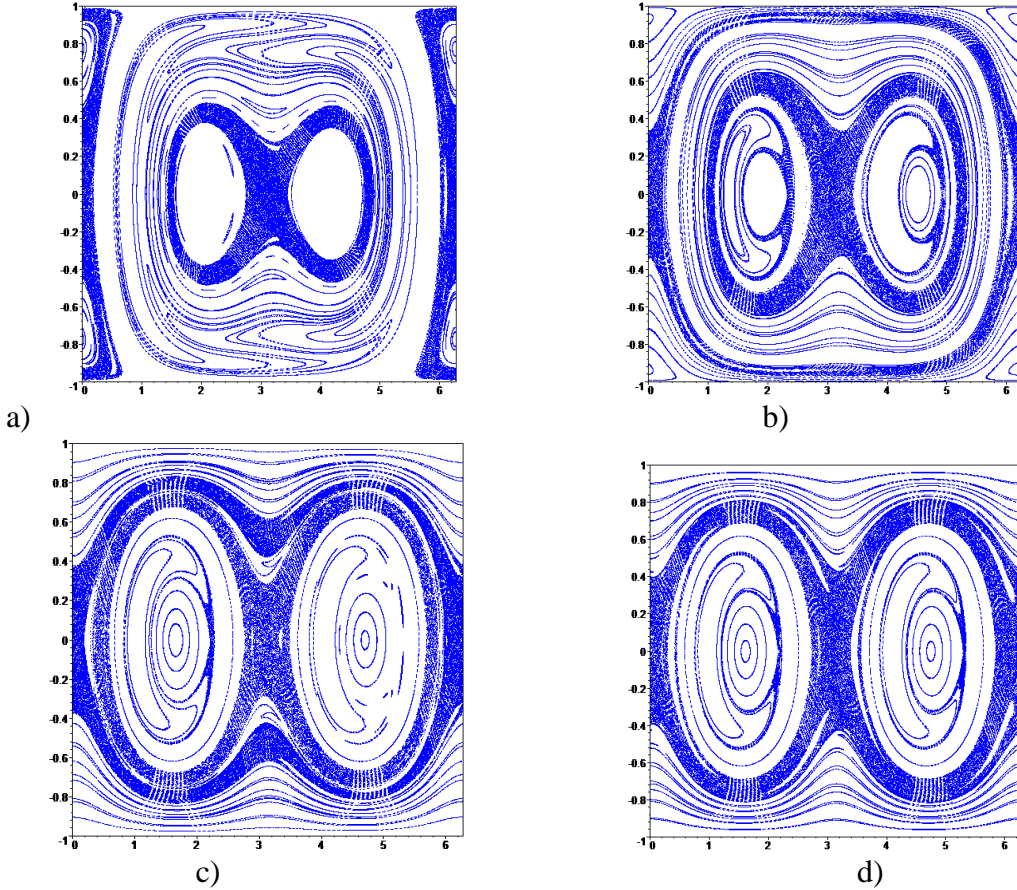


Figure 6. The Poincaré sections¹ of the dimensionless phase space $\{l, L/G\}$ for the SC with the triaxial inertia tensor at the following parameters²:

$$\hat{A} = 0.5, \quad \hat{B} = 0.6, \quad \hat{C} = 0.7; \quad G = 10; \quad D_{12} = D_{56} = 0; \quad \varepsilon = 0.01;$$

$$\text{a): } D_{34} = 0.9; \text{ b): } D_{34} = 0.5; \text{ c): } D_{34} = 0.1; \text{ d): } D_{34} = 0.01$$

¹ All of the presented in this work Poincaré sections were plotted with the help of the author's program complex [51].

² All of the parameters have numerical values corresponding to their own natural dimensions in the SI metric system.

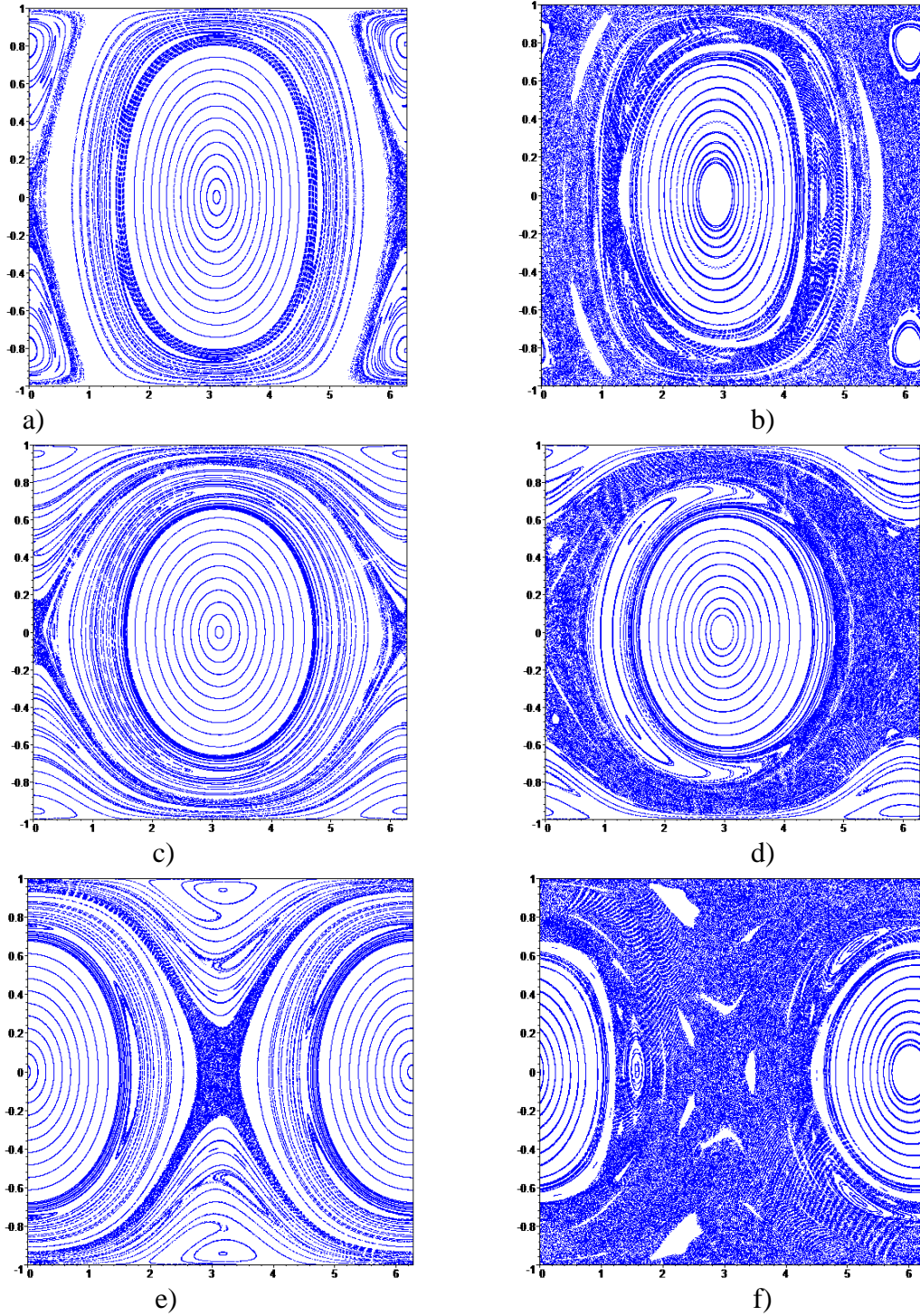


Figure 7. The Poincaré sections of the dimensionless phase space $\{l, L/G\}$ for the SC with the dynamical symmetry:

$$G = 3; \quad D_{12} = D_{56} = 0;$$

$$\text{a)-d): } \hat{A} = \hat{B} = 0.5, \quad \hat{C} = 0.7; \quad \text{e)-f): } \hat{A} = \hat{B} = 0.6, \quad \hat{C} = 0.4;$$

$$\text{a): } D_{34} = 0.5; \quad \varepsilon = 0.01; \quad \text{b): } D_{34} = 0.5; \quad \varepsilon = 0.1; \quad \text{c): } D_{34} = 0.25; \quad \varepsilon = 0.01; \quad \text{d): } D_{34} = 0.25; \quad \varepsilon = 0.1;$$

$$\text{e): } D_{34} = 0.5; \quad \varepsilon = 0.01; \quad \text{f): } D_{34} = 0.5; \quad \varepsilon = 0.1$$

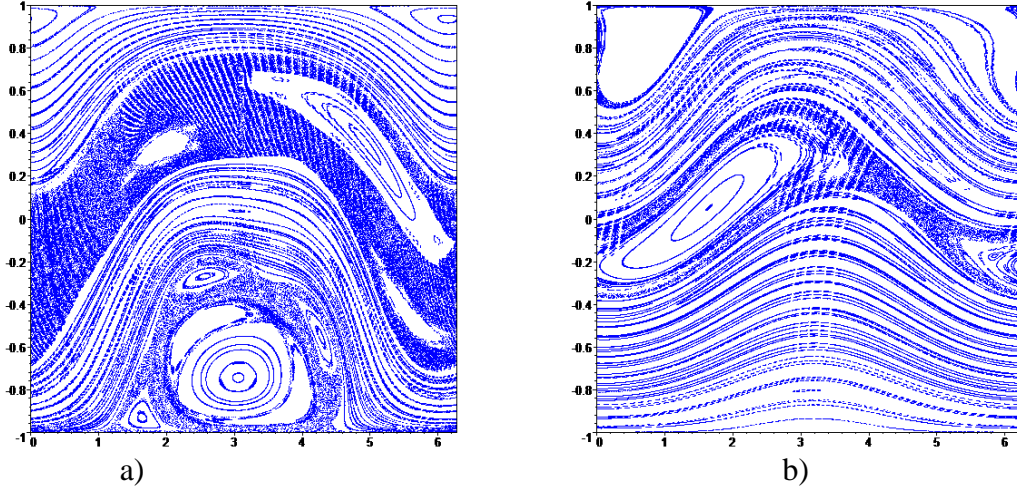


Figure 8. The Poincaré sections of the dimensionless phase space $\{l, L/G\}$

at all non-zero rotors' angular momentums:

$$G=3; D_{12}=0.5; D_{34}=0.6; D_{56}=1.5; \varepsilon=0.05;$$

$$\text{a): } \hat{A}=0.6; \hat{B}=0.7; \hat{C}=0.9; \quad \text{b): } \hat{A}=\hat{B}=0.6, \hat{C}=0.4;$$

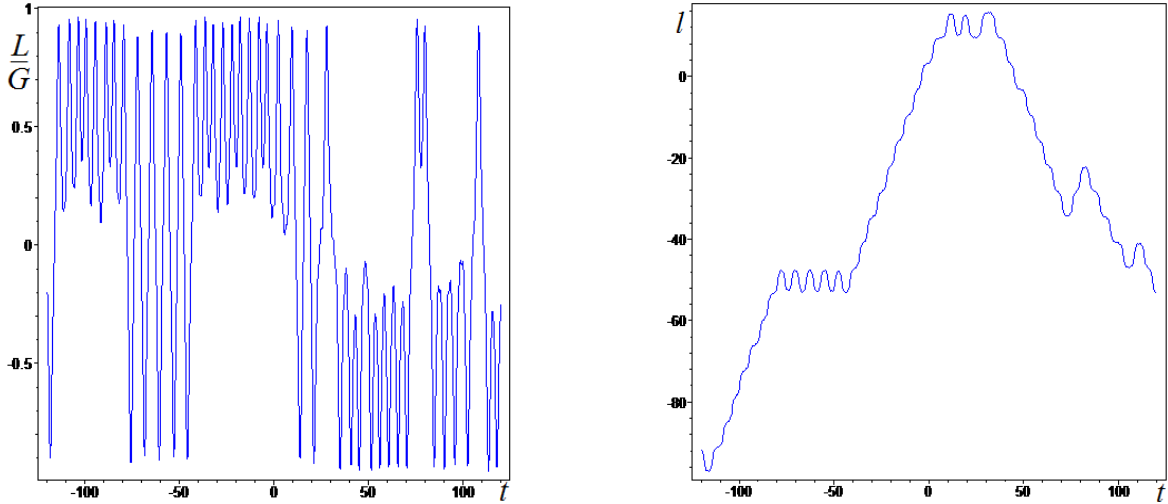


Figure 9. Irregular time-dependencies for the chaotic motion parameters

$$G=3; D_{12}=0; D_{34}=0.5; D_{56}=0; \varepsilon=0.1;$$

$$\hat{A}=\hat{B}=0.6, \hat{C}=0.4;$$

Presented above phase portraits (Poincaré sections) in the dimensionless space $\{l, L/G\}$ are very informative and fully describe dynamics of SC in the sense of quality of motion regimes; and also any point of these portraits can explain [28, 29] the main properties of the current SC attitude in terms of the nutation angle ($\theta = \arccos(L/G)$) and the intrinsic rotation angle (l).

From the modelling results the important notations follow.

Firstly, the chaotic motion areas (chaotic layers) are presented in the phase portrait of the system (fig.6-8), and, moreover, these areas divide the phase portrait into separated zones. At increasing the value of perturbations (the value of the parameter ε) it is possible to see the effect of the extension of chaotic areas, as well as the merger of these areas into one big chaotic layer (at the fig.7 we can see this integration at

the transition from the frame 7-a to the frame 7-b, from 7-c to 7-d, and from 7-e to 7-f). But, here we need to mention that these areas can be separable from each other (in the dynamical sense, which means the impermeability of the area border for the phase trajectory). Also, e.g., it is important here to indicate corresponding irregular time-dependences of motion parameters (fig.9) for the chaotic regime from the chaotic layer depicted at the figure 7-f.

Secondly, the modelling results demonstrate the presence of additional chaotic layers close to the secondary homo/heteroclinic structures arising in addition to the main separatrix-regions at the presence of perturbations. These secondary chaotic homo/heteroclinic bundles (“secondary chaos”) have properties similar to the main homo/heteroclinic chaos, and also must be taken into account at the formation of SC dynamics.

In the third, bifurcations of types of the phase portrait take place (from the fragment fig.6-a to 6-b, 6-c, 6-d successively) at the changing value of the equatorial rotors’ angular momentum (D_{34}); and we can also indicate the corresponding change of homo/heteroclinic bundles with chaotic layers – so, we should mention that at the transition to small values of equatorial angular momentum we take as the result, in fact, the phase portrait of the dual-spin SC with the longitudinal angular momentum (fig.6-d).

Also it is worth to note the complexity of the phase portrait structure (fig.8) of the SC perturbed motion at the non-zero angular momentums of rotors in all three main directions; here we see the strong deformation of the phase portrait form in comparison with previous results for equatorial rotors angular momentums (fig.6, 7), with arising of secondary chaotic layers.

5. Conclusion. So, the exact explicit polyharmonic form of the Melnikov function in considered case analytically proves the fact of splitting and multiple intersecting stable and unstable manifolds of the initial homoclinic separatrix-trajectory and the fact of local homoclinic chaos arising. Therefore the SC

dynamics will be liable to the homoclinic chaotization, that is the main reason of the SC tilting motion with disrupting the space mission. This fact must be taken into engineers’ attention at the space mission preparation and at the choice of working areas of SC dynamical parameters.

Acknowledgments

This work is partially supported by the Russian Foundation for Basic Research (RFBR#15-08-05934-A), and by the Ministry education and science of the Russian Federation (in the framework of the design part of the State Assignments to higher education institutions and research organizations in the field of scientific activity – project #9.1004.2014/K).

References

- [1] Golubev, V.V. (1953), Lectures on Integration of the Equations of Motion of a Rigid Body about a Fixed Point. Moscow: State Publishing House of Theoretical Literature.
- [2] Wittenburg, J. (1977), Dynamics of Systems of Rigid Bodies. Stuttgart: Teubner.
- [3] Wittenburg, J. (1975), Beitrage zur dynamik von gyrostaten, Accademia Nazionale dei Lincei, Quaderno N. 227.
- [4] Arkhangelski, U.A. (1977), Analytical rigid body dynamics, Nauka, Moscow, Russia.
- [5] Leimanis, E. (1965), The general problem of the motion of coupled rigid bodies about a fixed point. Berlin: Springer-Verlag.
- [6] Andoyer, H. (1923), Cours de Mecanique Celeste, Paris: Gauthier-Villars.
- [7] Deprit, A. (1967), A free rotation of a rigid body studied in the phase plane, American Journal of Physics no. 35, pp. 424 – 428.
- [8] Kinsey, K.J., Mingori, D.L. and Rand, R.H. (1996), Non-linear control of dual-spin spacecraft during despin through precession phase lock, J. Guidance Control Dyn., no. 19, pp. 60-67.
- [9] Nazari, M., and Butcher, E.A. (2014), On the stability and bifurcation analysis of dual-spin spacecraft, Acta Astronautica, vol. 93, pp. 162–175.
- [10] Sandfry, R.A. and Hall C.D. (2007), Bifurcations of relative equilibria of an oblate gyrost with a discrete damper, Nonlinear Dyn., vol. 48, pp. 319–329.
- [11] Burov, A.A. (2013), Conservative methods of controlling the rotation of a gyrost, Journal of Applied Mathematics and Mechanics, no. 77, pp. 195– 204.
- [12] Ivin, E.A. (1985), Decomposition of variables in

task about gyrostat motion, Mathematics and Mechanics series, Vestnik MGU (Transactions of Moscow's University), no. 3, pp. 69–72.

[13] Gutnik, S.A. and Sarychev, V.A. (2014), Dynamics of an axisymmetric gyrostat satellite. Equilibrium positions and their stability, Journal of Applied Mathematics and Mechanics, no. 78, pp. 249–257.

[14] Awad El-Gohary (2006), New control laws for stabilization of a rigid body motion using rotors system, Mechanics Research Communications, vol. 33, issue 6, pp. 818-829.

[15] Chaikin, S.V. (2013), Bifurcations of the relative equilibria of a gyrostat satellite for a special case of the alignment of its gyrostatic moment, Journal of Applied Mathematics and Mechanics, no. 77, pp. 477–485.

[16] Doroshin, A.V. (2008), Evolution of the Precessional Motion of Unbalanced Gyrostats of Variable Structure. Journal of Applied Mathematics and Mechanics, no. 72, pp. 259–269.

[17] Doroshin, A.V. (2010), Analysis of attitude motion evolutions of variable mass gyrostats and coaxial rigid bodies system, International Journal of Non-Linear Mechanics, vol. 45, issue 2, pp. 193–205.

[18] Doroshin, A.V. Attitude Control of Spider-type Multiple-rotor Rigid Bodies Systems. Proceedings of the World Congress on Engineering 2009, London, U.K., vol. II, pp. 1544-1549.

[19] Doroshin, A.V. (2014), Homoclinic solutions and motion chaotization in attitude dynamics of a multi-spin spacecraft, Communications in Nonlinear Science and Numerical Simulation, vol. 19, issue 7, pp. 2528–2552.

[20] Doroshin, A.V. (2011), Modeling of chaotic motion of gyrostats in resistant environment on the base of dynamical systems with strange attractors, Communications in Nonlinear Science and Numerical Simulation, vol. 16, issue 8, pp. 3188–3202.

[21] Doroshin, A.V. (2014), Chaos and its avoidance in spinup dynamics of an axial dual-spin spacecraft, Acta Astronautica, vol. 94, issue 2, pp. 563-576.

[22] Volterra, V. (1899), Sur la théorie des variations des latitudes. Acta Math., no. 22.

[23] Zhykovski, N.E. (1949), On the motion of a rigid body with cavities filled with a homogeneous liquid. Collected works, 1, Moscow-Leningrad, Gostekhisdat.

[24] Elipe, A. and Lanchares, V. (2008), Exact solution of a triaxial gyrostat with one rotor, Celestial Mechanics and Dynamical Astronomy, vol. 101, issue 1-2, pp. 49-68.

[25] Basak, I. (2009), Explicit solution of the Zhukovski-Volterra gyrostat, Regular and chaotic dynamics, vol.14, no. 2, pp. 223-236.

[26] Aslanov, V.S., Behavior of Axial Dual-spin Spacecraft, Proceedings of the World Congress on Engineering 2011, WCE 2011, 6-8 July, 2011, London, U.K., pp. 13-18.

[27] Aslanov, V.S. (2012), Integrable cases in the

dynamics of axial gyrostats and adiabatic invariants, Nonlinear Dynamics, vol. 68, no. 1-2, pp. 259-273.

[28] Doroshin, A.V. (2013), Exact solutions for angular motion of coaxial bodies and attitude dynamics of gyrostat-satellites. International Journal of Non-Linear Mechanics, vol. 50, pp. 68-74.

[29] Doroshin, A.V. (2013), Exact Solutions in Attitude Dynamics of a Magnetic Dual-Spin Spacecraft and a Generalization of the Lagrange Top, WSEAS Transactions on systems, vol. 12, issue 10, pp. 471-482.

[30] Jinlu Kuang, Soonhie Tan, Kandiah Arichandran and A.Y.T. Leung (2001), Chaotic dynamics of an asymmetrical gyrostat, International Journal of Non-Linear Mechanics, vol. 36, issue 8, pp. 1213-1233.

[31] Aslanov, V.S. and Doroshin, A.V. (2010), Chaotic dynamics of an unbalanced gyrostat. Journal of Applied Mathematics and Mechanics, vol. 74, issue 5, pp. 525-535.

[32] Doroshin, A.V. (2012), Heteroclinic dynamics and attitude motion chaotization of coaxial bodies and dual-spin spacecraft, Communications in Nonlinear Science and Numerical Simulation, vol. 17, issue 3, pp. 1460–1474.

[33] Doroshin, A.V. and Krikunov M.M. (2014), Attitude Dynamics of a Spacecraft with Variable Structure at Presence of Harmonic Perturbations, Appl. Math. Modelling, vol. 38, issues 7-8, pp. 2073-2089.

[34] Tabor, M. (1989), Chaos and Integrability in Nonlinear Dynamics: An Introduction. Wiley, John & Sons, New York.

[35] Melnikov, V.K. (1963), On the stability of the centre for time-periodic perturbations, Trans. Moscow Math. Soc., no.12, pp. 1-57.

[36] Wiggins, S. (1992), Chaotic Transport in Dynamical System. Springer-Verlag.

[37] Holmes, P. J. and J. E. Marsden (1983), Horseshoes and Arnold diffusion for Hamiltonian systems on Lie groups, Indiana Univ. Math. J., no. 32, pp. 273-309.

[38] Inarrea, M. and Lanchares, V. (2000), Chaos in the reorientation process of a dual-spin spacecraft with time-dependent moments of inertia, Int. J. Bifurcation and Chaos., no. 10, pp. 997-1018.

[39] Lin Yiing-Yuh and Wang Chin-Tzuo (2014), Detumbling of a rigid spacecraft via torque wheel assisted gyroscopic motion, Acta Astronautica, no. 93, pp. 1–12.

[40] Shirazi, K.H. and Ghaffari-Saadat, M.H. (2004), Chaotic motion in a class of asymmetrical Kelvin type gyrostat satellite, International Journal of Non-Linear Mechanics, vol. 39, issue 5, pp. 785-793.

[41] Doroshin, A.V. (2011), Modeling of chaotic motion of gyrostats in resistant environment on the base of dynamical systems with strange attractors. Communications in Nonlinear Science and Numerical Simulation, vol. 16, issue 8, pp. 3188–3202.

[42] El-Gohary Awad (2009), Chaos and optimal control of steady-state rotation of a satellite-gyrostat on a circular orbit, Chaos, Solitons & Fractals, vol. 42, pp.

2842-2851.

[43] Boccaletti, S., Kurths, J., Osipov, G., Valladares, D.L. and Zhou, C.S. (2002), The synchronization of chaotic systems. *Physics Reports*, no. 366, pp. 1-101.

[44] Anishchenko, V.S., Astakhov, V.V., Neiman, A.B., Vadivasova, T.E. and Schimansky-Geier, L. (2007), *Nonlinear Dynamics of Chaotic and Stochastic Systems. Tutorial and Modern Development*. Springer-Verlag, Berlin.

[45] Beletskii, V.V., Pivovarov, M.L. and Starostin, E.L. (1996), Regular and chaotic motions in applied dynamics of a rigid body, *Chaos*, vol. 6, no. 2.

[46] solarsystem.nasa.gov/missions/docs/galileo-end.pdf

[47] www.boeing.com/history/products/376-satellite.page

[48] www.astronautix.com/craft/hs376.htm

[49] hubblesite.org/

[50] www.nasa.gov/mission_pages/kepler/main/index.html

[51] Doroshin, A.V., The program complex for the analysis of dynamical systems // Certificate of registration of the computer program in the Russian Federation register of programs №2008613358 - 16.07.2008.

А.В. Дорошин

Самарский государственный
аэрокосмический университет
имени академика С. П. Королёва
(национальный исследовательский
университет)
443086, Россия, г. Самара,
Московское шоссе, 34
doran@inbox.ru
doroshin@ssau.ru

ОБРАЗЫ ХАОСА В ДИНАМИКЕ УГЛОВОГО ДВИЖЕНИЯ МНОГОРОТОРНЫХ КОСМИЧЕСКИХ АППАРАТОВ И СПУТНИКОВ-ГИРОСТАТОВ

Изучаются аспекты хаотической динамики многороторных аппаратов и спутников-гиростатов. Исследования проводятся с помощью метода Мельникова и сечений Пуанкаре. Образы динамического хаоса строятся для разнообразных фазовых портретов, соответствующих различным величинам динамических параметров. Иллюстрируются бифуркации хаотических режимов с изменением структуры фазовых портретов.

Ключевые слова: многороторные механические системы, космический аппарат с двойным вращением, космический аппарат со множественным вращением, гиростат, гомоклинический хаос, полигармонические возмущения, функция Мельникова, сечение Пуанкаре.